JOURNAL OF GEOPHYSICAL RESEARCH: SPACE PHYSICS, VOL. 119, 479–489, doi:10.1002/2013JA018974, 2014

Numerical simulations of compact intracloud discharges as the Relativistic Runaway Electron Avalanche-Extensive Air Shower process

S. Arabshahi,[1] J. R. Dwyer,[1] A. Nag,[2,3] V. A. Rakov,[2] and H. K. Rassoul[1]

Received 3 May 2013; revised 29 November 2013; accepted 4 December 2013; published 16 January 2014.

[1] Compact intracloud discharges (CIDs) are sources of the powerful, often isolated radio pulses emitted by thunderstorms. The VLF-LF radio pulses are called narrow bipolar pulses (NBPs). It is still not clear how CIDs are produced, but two categories of theoretical models that have previously been considered are the Transmission Line (TL) model and the Relativistic Runaway Electron Avalanche-Extensive Air Showers (RREA-EAS) model. In this paper, we perform numerical calculations of RREA-EASs for various electric field configurations inside thunderstorms. The results of these calculations are compared to results from the other models and to the experimental data. Our analysis shows that different theoretical models predict different fundamental characteristics for CIDs. Therefore, many previously published properties of CIDs are highly model dependent. This is because of the fact that measurements of the radiation field usually provide information about the current moment of the source, and different physical models with different discharge currents could have the same current moment. We have also found that although the RREA-EAS model could explain the current moments of CIDs, the required electric fields in the thundercloud are rather large and may not be realistic. Furthermore, the production of NBPs from RREA-EAS requires very energetic primary cosmic ray particles, not observed in nature. If such ultrahigh-energy particles were responsible for NBPs, then they should be far less frequent than is actually observed.

Citation: Arabshahi, S., J. R. Dwyer, A. Nag, V. A. Rakov, and H. K. Rassoul (2014), Numerical simulations of compact intracloud discharges as the relativistic Runaway Electron Avalanche-Extensive Air Shower process, *J. Geophys. Res. Space Physics*, *119*, 479–489, doi:10.1002/2013JA018974.

1. Introduction

[2] In recent years there have been several efforts to explain the most powerful natural HF-VHF radio emitters on Earth, called compact intracloud discharges (CIDs) or narrow bipolar events (NBEs) [*Le Vine*, 1980; *Smith et al.*, 1999]. The peak radiated power of these events in the 60–66 MHz frequency range can exceed 300 kW [*Thomas et al.*, 2001]. The associated VLF-LF radio pulses (sferics) are called narrow bipolar pulses (NBPs) [*Smith et al.*, 1999]. In this paper, we use the physics sign convention with the positive direction pointed upward. Generally, the polarity of the NBPs should be opposite to that of the electrostatic field in the discharge region. The observations are consistent with this assumption, and they have shown that the source altitudes of the negative narrow bipolar pulses (NNBPs) tend to be located at the top of the upper positive region in the standard cloud model where the electrostatic field is directed upward. In the standard model, the cloud has a tripole polarity with the upper positive charge in the top, negative charge in the midlevel region, and a smaller positive charge in the lower part of the cloud [*Rakov and Uman*, 2004]. In terms of their waveform, they usually appear as either a narrow positive half cycle followed by a smaller but longer negative overshoot, called positive narrow bipolar pulses (PNBPs), or a narrow negative half cycle followed by a smaller, but longer positive overshoot, called negative narrow bipolar pulses (NNBPs) [*Willett et al.*, 1989]. NBPs last for about 10–30 μs, with the initial rise plus fall time of 5–10 μs [*Smith et al.*, 2002; *Nag et al.*, 2010]. They are known to be associated with strong convection in thunderstorms and have altitudes of about 15–19 km for NNBPs and 8–15 km for PNBPs [*Smith et al.*, 2004; *Wu et al.*, 2012] (see *Lü et al.* [2013, Table 3] for a recent review). This suggests that NNBPs may be produced above the main positive charge layer and PNBPs may be produced between the main positive charge and main negative charge layers.

[3] Interestingly, NBPs do not seem to be associated with return strokes of cloud-to-ground (CG) lightning discharges. They often appear as large isolated (at least within ten to

[1]Department of Physics and Space Sciences, Florida Institute of Technology, Melbourne, Florida, USA.
[2]Department of Electrical and Computer Engineering, University of Florida, Gainesville, Florida, USA.
[3]Now at Vaisala, Inc., Louisville, Colorado, USA.

Corresponding author: S. Arabshahi, Department of Physics and Space Sciences, Florida Institute of Technology, 150 W. University Blvd., Melbourne, FL 32901, USA. (sarabshahi2009@my.fit.edu)

2169-9380/14/10.1002/2013JA018974

hundreds of milliseconds [*Nag et al.*, 2010]) bipolar pulses with no apparent leader activity beforehand. There are also strong HF-VHF emissions superimposed on *E* and *B* field waveforms. Throughout the rest of this paper we will refer to NBPs as the low-frequency (LF) bipolar waveform or sferic. The strong HF-VHF emissions are an important part of the process, and any successful model must include these emissions. However, investigating these emissions is beyond the scope of this study.

[4] Different models have been developed to explain NBPs. These models are mainly developed assuming an existing conductive channel. However, a number of discrepancies exists between these models, and creation of the conductive channel remains an open question. The goal of the present work is to compare the results of some of the previously proposed models of CIDs and present some new insights into the properties of these events.

2. Review of CID Models

[5] Most of the theoretical models that explain the NBPs fall into two distinct categories: the group of different versions of the Transmission Line (TL) model or the relativistic Runaway Electron Avalanche-Extensive Air Showers (RREA-EAS) model group. In the following sections we will review the basic ideas behind these two theoretical models and then compare the predictions of these models.

2.1. Transmission Line Model

[6] The detailed physical mechanism that can produce CIDs is still unknown. In order to better understand and analyze these events, scientists usually assume a current wave propagating along a hot conductive channel. However, there is no explanation of how such a highly conductive channel could quickly form. Such models are referred here as the Transmission Line (TL)-type models. TL model has been widely used in the form of either a single traveling wave [*Watson and Marshall*, 2007; *Uman et al.*, 1975; *Zhu et al.*, 2010] or a wave folding on itself while being reflected from the ends of the channel (bouncing wave model) [*Nag and Rakov*, 2009, 2010a; *Hamlin et al.*, 2007].

[7] In 2007, *Watson and Marshall* [2007], for a set of data measured by *Eack* [2004], compared the results of the TL model with two modified versions of the model called Modified Transmission Line Exponentially Increasing (MTLEI) with negative charge carriers and MTLEI model with positive charge carriers. They set the current to have a time dependency of the following form:

$$i(t) = \begin{cases} Ae^{-(\alpha(t-t_1))^2} & t \le t_1 \\ Ae^{-(\alpha(t-t_1)/k)^2} & t_1 \le t \end{cases}, \tag{1}$$

where A, k, and α are constants and can be found by matching the model with the data. They then introduced three models for the propagation of the current pulse along the conductive channel in the following forms:

[8] 1. TL model

$$i(z,t) = i\left(t - \frac{z - H_1}{v}\right), \tag{2}$$

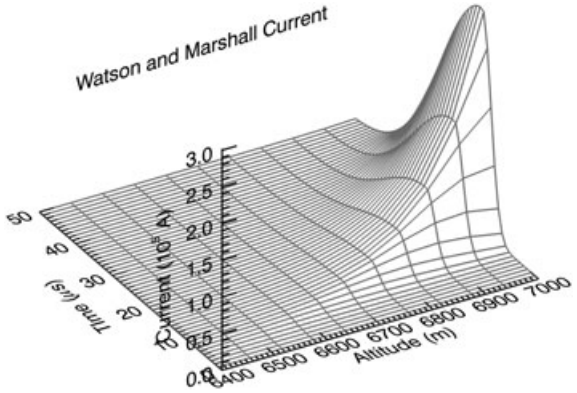

Figure 1. Current pulse used in *Watson and Marshall* [2007].

[9] 2. MTLEI with negative charge carriers

$$i(z,t) = e^{(z-H_1)/\lambda} i\left(t - \frac{z - H_1}{v}\right), \tag{3}$$

[10] 3. MTLEI with positive charge carriers

$$i(z,t) = e^{(H_2-z)/\lambda} i\left(t - \frac{H_2 - z}{v}\right), \tag{4}$$

where H_1 and H_2 are the heights of the bottom and top of the conductive channel, respectively, v is the propagation speed of the current pulse along the conductive channel, and λ is the growth rate of the current pulse. These constants can be found by fitting the model to the experimental data. *Watson and Marshall* [2007] showed that the MTLEI with negative charge carriers would fit the best to the measured data of positive NBPs in *Eack* [2004]. Figure 1 shows the 3-D representation of the reproduction of the current pulse used in *Watson and Marshall* [2007] for the MTLEI with negative charge carriers model. Based on the results from the simulations, *Watson and Marshall* [2007] suggested that a process similar to the runaway breakdown process could be giving rise to NBPs. In the same study, the authors conclude that the electrons, not the ions, are the charge carriers for the propagation of the current pulse.

[11] On the basis of experimental evidence of multiple reflections and modeling, *Nag and Rakov* [2010a] inferred that, from the electromagnetic point of view, the CID is essentially a bouncing wave phenomenon. The process can be viewed as a long wave repeatedly folding on itself, so that the electromagnetic field signature (narrow bipolar pulse) duration is not necessarily a measure of radiator length. Reflections at channel extremities may result in corona-like electrical breakdown there, because a reduction of current is accompanied by an increase of line charge density and associated voltage. This breakdown at channel ends is likely to produce intense bursts of HF-VHF radiation which are a characteristic feature of CIDs. *Nag and Rakov* [2010a] showed via modeling that reflections were responsible for fine structure of wideband electric field and dE/dt waveforms. From modeling the CID as a wave traveling on an elevated vertical transmission line and comparing model-predicted electric fields with measurements, they estimated that the effective current reflection coefficients at channel ends (additionally accounting for current attenuation along

the channel) should be in the range of 0 to –0.5, that the wave propagation speed ranges from 0.3 to 3×10^8 m/s, and the channel length is less than 1000 m. Further, *Nag and Rakov* [2010a] showed that the current distribution along the CID channel is often not much different from uniform, as expected for a Hertzian (electrically short) dipole, because of relatively short channel length, relatively long current waveform, and relatively high propagation speed. Both the bouncing wave model and the Hertzian dipole approximations were shown to be capable of reproducing two-station CID electric field measurements of *Eack* [2004].

[12] *Nag and Rakov* [2010b] estimated electrical parameters of 48 located CIDs using their measured electric fields and vertical Hertzian dipole approximation. For all 48 events, geometric mean values of peak current, zero-to-peak current risetime, and charge transfer for the first 5 μs were inferred to be 74 kA, 5 μs, and 164 mC, respectively. The geometric mean peak radiated power, and energy radiated for the first 5 μs were 29 GW and 31 kJ, respectively. For nine events, they were able to estimate CID channel length from channel traversal times measured in dE/dt waveforms and assumed propagation speeds of 2×10^8 m/s to 3×10^8 m/s, which limit the range of allowed speed values. For $v = 2.5 \times 10^8$ m/s (average value), the channel lengths for these nine events ranged from 108 to 142 m. The corresponding geometric mean values of peak current, zero-to-peak current risetime, and charge transfer for the first 5 μs are 143 kA, 5.4 μs, and 303 mC, respectively. The uncertainty in either current or charge transfer calculated for the nine events was estimated to be $\leq$ 25%. The geometric mean peak radiated power and energy radiated for the first 5 μs (both wideband) were calculated to be 29 GW and 24 kJ, respectively. Overall, the estimated CID current waveform parameters were found to be comparable to their counterparts for first strokes in cloud-to-ground lightning, while their peak radiated electromagnetic power was considerably higher.

[13] In case of the PNBPs, their source altitudes are consistent within the region between the main positive and the main negative regions of the standard cloud model where the electric field is downward. All three events examined here are of this type, although source altitudes for two of them are too high to be consistent with the standard cloud model.

[14] Although the TL-type models do not have a good explanation of what could be the cause of such strong discharges, they can explain some of the main characteristics of NBPs. In the next section we will examine one of the proposed models that claims to be able to explain the occurrence of NBPs. A critical review of another model of this type is found in Appendix B.

2.2. RREA-EAS Model

[15] It has been proposed that NBPs are caused by the development of a conductive channel with the help of Relativistic Runaway Electron Avalanches seeded by cosmic ray air showers, called the RREA-EAS model, also referred to as the Runaway Breakdown-EAS model [*Gurevich et al.*, 2013, 2004; *Gurevich and Zybin*, 2004; *Gurevich et al.*, 2002, 2009]. We know that when high-energy cosmic ray particles (e.g., electrons, positrons, and muons) travel through a region of atmosphere in which the ambient electric field is greater than the runaway electron avalanche threshold, they would act as seed particles for Relativistic Runaway Electron Avalanches (RREAs) [*Gurevich and Zybin*, 2004]. The current from these avalanches does not require the presence of a hot conductive channel, and it is not clear if they can produce a hot channel [*Dwyer and Babich*, 2012]. Instead, runaway electrons produce a large number of low-energy electrons by ionizing the air. The low-energy electrons then drift in the thunderstorm electric field producing electric currents and radio frequency emissions [*Dwyer et al.*, 2009]. It has been suggested that these RF emissions could account for NBPs [*Gurevich and Zybin*, 2004]. The polarity of these emissions would be determined by the direction of the electrostatic field at their source. Here we will show the results of CID simulations based on the RREA-EAS model and will compare the results with measurements of NBPs.

[16] Runaway electrons produced by high-energy air shower particles can produce low-energy positive and negative ions, low-energy electrons, and more high-energy electrons through the ionization of the air. However, as has been shown in *Dwyer et al.* [2009], the low-energy ions do not contribute significantly to the current density distribution. So the total current density including both high-energy and low-energy electrons contribution is

$$\vec{J}(x,y,z,t) = \vec{v}_{\mathrm{le}}\rho_{\mathrm{le}}(x,y,z,t) + \vec{v}_{\mathrm{re}}\rho_{\mathrm{re}}(x,y,z,t), \tag{5}$$

where $\rho_{\mathrm{le}}(x,y,z,t)$, $\vec{v}_{\mathrm{le}}$, $\rho_{\mathrm{re}}(x,y,z,t)$, and $\vec{v}_{\mathrm{re}}$ are charge density and velocity of low-energy and high-energy electrons, respectively. The first term on the right-hand side is the current due to low-energy electrons, and the second term is due to runaway (high-energy) electrons. In the following two subsections we will find the contribution due to each term to the total current.

2.2.1. Energetic Runaway Electrons

[17] For an arbitrary electric field, the density of runaway electrons is approximately given by the general transport equation [*Dwyer*, 2010]

$$\frac{\partial n_{\mathrm{re}}}{\partial t} + \vec{\nabla}\cdot(\vec{v}_{\mathrm{re}}n_{\mathrm{re}}) - \vec{\nabla}\cdot(\hat{D}\cdot\vec{\nabla}n_{\mathrm{re}}) - \frac{n_{\mathrm{re}}}{\tau} = n_s, \tag{6}$$

where n_s is the source function describing the number of seed particles per second per cubic meter, and $\vec{v}_{\mathrm{re}}$ is the average velocity of the runaway electrons [*Gurevich and Zybin*, 2001; *Dwyer*, 2005]. The average speed of the avalanche was calculated by *Coleman and Dwyer* [2006] and it is approximately 0.89c . The third term on the left-hand side describes the diffusion of energetic electrons. If we ignore the lateral profile of the avalanche and consider just the propagation along the longitudinal direction, equation (6) could be written as follows:

$$\frac{\partial n_{\mathrm{re}}}{\partial t} + \frac{\partial}{\partial z}(\vec{v}_{\mathrm{re}}n_{\mathrm{re}}) - \frac{\partial}{\partial z}\left(D_{\parallel}\frac{\partial n_{\mathrm{re}}}{\partial z}\right) - \frac{n_{\mathrm{re}}}{\tau} = n_s. \tag{7}$$

This one-dimensional representation of the general transport equation (6) is sufficient for calculations of the LF/VLF electromagnetic emissions, since the lateral distribution has a small effect on the result.

[18] The last term on the left-hand side of equation (7) describes the avalanche multiplication, with τ being the avalanche e-folding time. The avalanche e-folding time can be derived using the following empirical equation:

$$v\tau \approx \lambda = \frac{7300\ \mathrm{kV}}{(E - 276\ \mathrm{kV/m} \times n)}, \tag{8}$$

Table 1. Parameters of Three CIDs Recorded at the Lightning Observatory in Gainesville, Florida in 2008

Event ID	Horizontal Distance to the Antenna D (km)	Source Altitude h (km)	Inclined Distance to the Antenna R (km)
082308_163	68	19	71
082308_164	64	16	66
091108_175	36	8.9	37

where E is the background electric field measured in kV/m, v is the speed of the avalanche in m/s, λ is the e-folding length in meters, and n is the density of air relative to its value at sea level at STP [*Dwyer*, 2003; *Coleman and Dwyer*, 2006]. Equation (8), which is in good agreement with the avalanche length calculated by other authors [*Dwyer et al.*, 2012], remains a good approximation for all the electric fields in the cloud, including fields below the RREA threshold field. This is because of the exponential energy spectrum of the runaway electrons.

[19] In *Dwyer* [2010], it has been shown that for a uniform electric field along $-z$, the differential equation (7) has the following Green's function:

$$G_{\mathrm{re}}(x,y,z,t;x_0,y_0,z_0,t_0) = \frac{1}{\sqrt{4\pi(t-t_0)D_{\parallel}}} \cdot \exp\left(\frac{(t-t_0)}{\tau} - \frac{(v_{\mathrm{re}}(t-t_0)-(z-z_0))^2}{4D_{\parallel}(t-t_0)}\right) \cdot S(t-t_0)\delta(x-x_0)\delta(y-y_0)S(z_0)S(L-z). \quad (9)$$

The step function, S, guarantees that only locations within the avalanche region ($0 < z < L$) are considered and that the avalanche propagates in the correct direction, opposite the electric field vector. The step function, $S(x)$ is defined to be equal to 0 for $x < 0$ and equal to 1 for $x \geq 0$.

[20] In the appendix of this paper we have shown that for a nonuniform electric field along $-z$ we would have the following Green's function for equation (7):

$$G_{\mathrm{re}}(x,y,z,t;x_0,y_0,z_0,t_0) = \frac{1}{\sqrt{4\pi(t-t_0)\overline{D}_{\parallel}(z,z_0)}} \times \exp\left(\int_{t_0}^{t}\frac{\mathrm{d}t}{\tau} - \frac{(v_{\mathrm{re}}(t-t_0)-(z-z_0))^2}{4(t-t_0)\overline{D}_{\parallel}(z,z_0)}\right) \cdot S(t-t_0)S(t-t_0)\delta(x-x_0)\delta(y-y_0)S(z_0)S(L-z), \quad (10)$$

where $\overline{D}_{\parallel}(z,z_0)$ is the averaged diffusion coefficient over the interval z_0 to z. In this equation τ is the e-folding time, and it is a function of the electric field. It can be calculated using equation (8).

[21] As a result, the solution for an arbitrary density of seed particles, n_s, can be found by integrating the Green's function (10) as follows:

$$n_{\mathrm{re}}(x,y,x,t) = \int\int\int\int G_{\mathrm{re}}(x,y,z,t;x_0,y_0,z_0,t_0) \cdot n_s(x_0,y_0,z_0,t_0)\,\mathrm{d}x_0\mathrm{d}y_0\mathrm{d}z_0\mathrm{d}t_0. \quad (11)$$

[22] The density of energetic seed particles is related to the number density of the energetic charged particles in the air shower as [*Dwyer et al.*, 2009]

$$n_s(x_0,y_0,z_0,t_0) = \frac{u}{\lambda}n_{\mathrm{EAS}}(x_0,y_0,z_0,t_0), \quad (12)$$

where u is the speed of the air shower in the thunderstorm. Due to the Lorentz contraction, the longitudinal thickness of the air shower is highly compressed compared to its lateral size. The density of the particles in the air shower is usually described as a thin pancake-like shape with a slight curvature. Since in this study we are not considering the lateral distribution of the runaway electrons, we shall ignore the lateral width of the shower as well. Therefore, the density of energetic particles in the shower can be written as follows:

$$n_{\mathrm{EAS}}(x_0,y_0,z_0,t_0) = N_{\mathrm{EAS}}\delta(u_x t_0 - x_0)\delta(u_z t_0 - z_0)\delta(y_0), \quad (13)$$

where N_{EAS} is the number of secondary charged particles in the air shower, and u_x, u_z are the horizontal and vertical components of the air shower core velocity. Since we are interested in the maximum number of runaway electrons that can be produced by air showers, we will assume a vertically moving air shower ($u_x = 0$, $u_z = u$). So,

$$n_{\mathrm{EAS}}(x_0,y_0,z_0,t_0) = N_{\mathrm{EAS}}\delta(x_0)\delta(ut_0 - z_0)\delta(y_0). \quad (14)$$

Finally, the density of runaway electrons can be written as follows:

$$n_{\mathrm{re}}(x,y,z,t) = \frac{uN_{\mathrm{EAS}}}{\lambda}\delta(x)\delta(y)\int \frac{1}{\sqrt{4\pi(t-t_0)\overline{D}_{\parallel}(z-ut_0)}} \cdot \exp\left(\int_{t_0}^{t}\frac{\mathrm{d}t}{\tau} - \frac{(v_{\mathrm{re}}(t-t_0)-(z-ut_0))^2}{4(t-t_0)\overline{D}_{\parallel}(z-ut_0)}\right) \cdot S(t-t_0)S(ut_0)S(L-z)\mathrm{d}t_0. \quad (15)$$

The charge density of the runaway electrons can be found using

$$\rho_{\mathrm{re}}(x,y,z,t) = -en_{\mathrm{re}}(x,y,z,t), \quad (16)$$

and the current due to the runaway electrons using

$$\vec{J}_{\mathrm{re}}(x,y,z,t) = \vec{v}_{\mathrm{re}}\rho_{\mathrm{re}}(x,y,z,t). \quad (17)$$

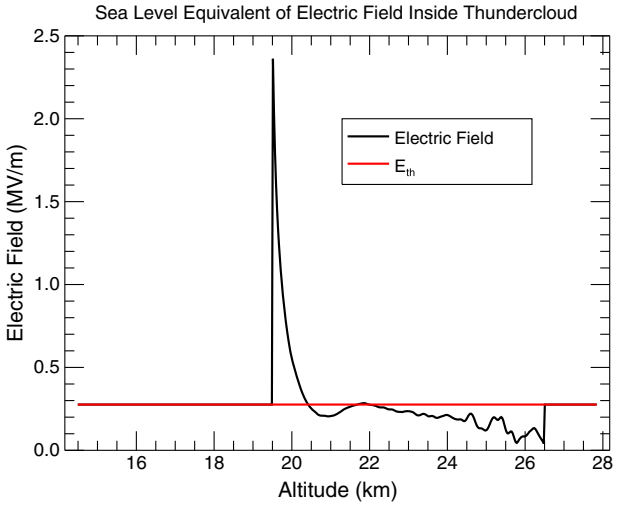

Figure 2. Thundercloud electrostatic field versus altitude (black curve) needed in our RREA-EAS model to match NBP ID 082308_163. The red line shows the RREA threshold field.

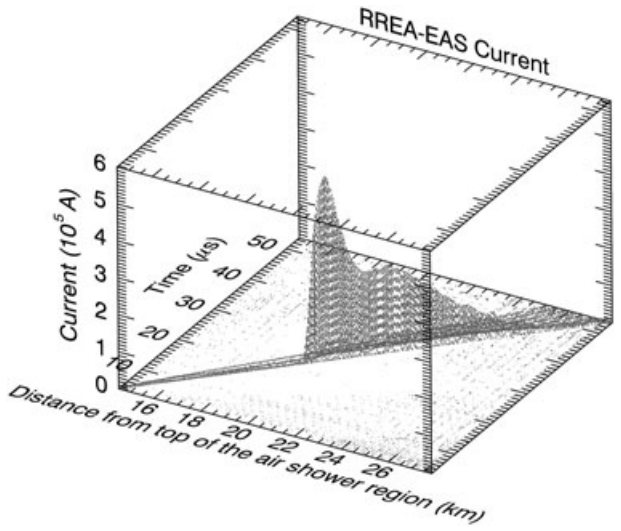

Figure 3. RREA-EAS model predicted current pulse that produced NBP ID 082308_163.

2.2.2. Low-Energy Electrons

[23] As the runaway electrons propagate, secondary electrons below the runaway threshold energy very rapidly lose energy through ionization of the air and produce low-energy electrons. The low-energy electrons will then quickly attach to the molecules of the air in time τ_a. Therefore, the charge density of the low-energy electrons can be calculated from [*Dwyer et al.*, 2009]

$$\frac{\mathrm{d}\rho_{\mathrm{le}}}{\mathrm{d}t} = -J_{\mathrm{re}} l - \frac{\rho_{\mathrm{le}}}{\tau_a}, \tag{18}$$

where l is the low-energy electron production rate, [1/m], [*Dwyer et al.*, 2009; *Dwyer and Babich*, 2011]. Equation (18) has the general solution:

$$\rho_{\mathrm{le}}(x,y,z,t) = -l \int_{-\infty}^{\infty} \exp\left(-(t-t'')/\tau_a\right) \cdot S(t-t'') J_{\mathrm{re}}(x,y,z,t'')\, \mathrm{d}t''. \tag{19}$$

[24] The low-energy electrons will drift in the electric field for a distance $d = v_{\mathrm{le}}\tau_a$. This distance depends on the electric field strength and the ambient air density, and it is typically on the order of a millimeter. Having the density of low-energy electrons, their current is

$$J_{\mathrm{le}} = v_{\mathrm{le}}\rho_{\mathrm{le}}. \tag{20}$$

3. Simulation Results

[25] In this section we will show the results of simulations of the RREA-EAS process for a few examples of NBP measurements. The initial conditions for the simulations have been found by matching the theoretical model to the experimentally measured data.

[26] The background electrostatic field is one of the required input parameters of the RREA-EAS model. In our simulations we have used a *Prediction-Correction Method* in order to find it. We first find the background electric field profile (required for model) by matching a measured waveform from a CID event to the simplified version of the RREA-EAS model. The *Prediction* will then calculate the *correct* sferic using the most realistic thundercloud parameters as input to the fully developed RREA-EAS model. Ultimately the simulated waveform can give us the characteristics of the CID and the energy of the cosmic ray particle that produced it.

[27] In order to predict the electrostatic field, we have assumed that the only significant term in the measured electric field pulse is the radiation term, and the lateral and longitudinal diffusion are negligible.

[28] The radiation term of the electric field produced by a current along the z axis measured on the ground is [e.g., *Uman*, 2001]

$$E_{\mathrm{rad}}(D,t) = -\int_{H_1}^{H_2} \frac{\sin^2\theta}{c^2 R} \frac{\partial j(z, t-R/c)}{\partial t}\, \mathrm{d}z. \tag{21}$$

In the lowest order approximation of the RREA-EAS model we assume a radiative point source. The source is moving along the z axis, and at the retarded time $t - R/c$ it has the following form:

$$j(z, t-R/c) = J(t-R/c)\delta\left(z - v_{\mathrm{re}} \times (t-R/c)\right). \tag{22}$$

Substituting the above equation (22) into the radiation field equation (21), the point source current can be derived as follows:

$$J(t-R/c) = \int_0^t \frac{c^2 R}{\sin^2\theta} E_{\mathrm{rad}}(D,t')\mathrm{d}t'. \tag{23}$$

This can be transformed to the source time as

$$J(t) = \int_0^{t+R/c} \frac{c^2 R}{\sin^2\theta} E_{\mathrm{rad}}(D,t')\mathrm{d}t'. \tag{24}$$

On the other hand, from the RREA-EAS theory we know that the total current of electrons is

$$J(t) = v_{\mathrm{re}}\rho_{\mathrm{re}}(t) + v_{\mathrm{le}}\rho_{\mathrm{le}}(t). \tag{25}$$

In the limit $\tau_a << \lambda/v_{\mathrm{re}}$ due to the same distribution of low-energy electrons and runaway electrons, we have [*Dwyer et al.*, 2009]

$$J(t) = (1 + l v_{\mathrm{le}}\tau_a) v_{\mathrm{re}}\rho_{\mathrm{re}}(t). \tag{26}$$

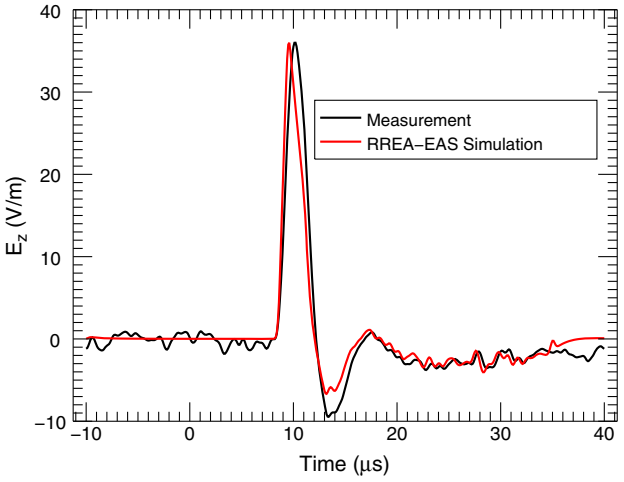

Figure 4. Comparison of measured E field waveform to the results from RREA-EAS model simulation.

Table 2. RREA-EAS Model Predicted Parameters for Three CIDs Listed in Table 1

Event ID	Initial Cosmic Ray Energy E_{CR} (eV)	Electrostatic Field Peak (MV/m)	Discharge Channel Length (km)	Peak Current (kA)	Discharge Speed
082308_163	6.06×10^{21}	2.36	13.21	502	$0.89c$[a]
082308_164	6.26×10^{21}	1.18	13.32	666	$0.89c$
091108_175	4.40×10^{21}	0.53	7.88	554	$0.89c$

[a] c is the speed of light.

The speed of low-energy electrons, v_{le}, and their attachment time depend on the air density and electric field inside the cloud. It can be calculated from

$$v_{le} = \mu E, \tag{27}$$

where μ is the mobility of electrons and E is the electrostatic field inside the cloud. For our simulations, we have used the theoretical model in *Morrow and Lowke* [1997] presented for the attachment time and mobility of electrons in the air.

[29] For the simplest model of the runaway electrons, the charge density has the following exponential form:

$$\rho_{re}(t) = \rho_0 \exp\left(\int_0^t \frac{v_{re}\mathrm{d}t'}{\lambda(t')}\right). \tag{28}$$

The time dependence of the current, $J(t)$, then can be written as

$$J(t) = (1 + lv_{le}\tau_a)v_{re}\rho_0 \exp\left(\int_0^t \frac{v_{re}\mathrm{d}t'}{\lambda(t')}\right), \tag{29}$$

where $\lambda(t)$ is the avalanche e-folding length. Simplifying equation (29), substituting the current from equation (24) into it, and using the e-folding length equation (8), the electric field inside the thundercloud can be derived by

$$E(z) = \left\{7300[\mathrm{kV}]\left[\frac{R\,E_{rad}(t + R/c)}{v_{re}\int_0^t R\,E_{rad}(t' + R/c)\mathrm{d}t'}\right] + E_{th}\right\} \times \delta(z - v_{re}t)[\mathrm{kV/m}]. \tag{30}$$

Equation (30) is the nonrelativistic version of the equation derived in *Dwyer et al.* [2009]. Nonrelativistic regime is a valid assumption since the observer is very far from the source, and the direction of the source to the observer is almost perpendicular to the direction of the current propagation. Knowing the electrostatic electric field inside the thundercloud, we can simulate the RREA-EAS process using the theory that includes almost all the physical characteristics that contribute to this process.

[30] Following on the *Prediction-Correction Method*, we will use the field from equation (30) to find the current pulse for the more detailed model of equations (15), (17), and (5). This will be the *Correction* part of the method. The radiation electric field, E_z, from the current pulse can then be calculated using the model for an arbitrary current along a vertically oriented finite antenna above a conducting plane

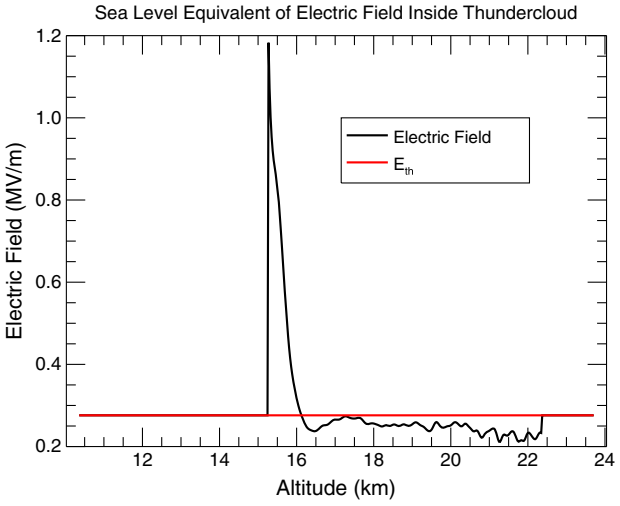

Figure 5. RREA-EAS model predicted electrostatic field inside thundercloud for NBP ID 082308_164.

described in *Uman et al.* [1975] and compared with the observations as a consistency test:

$$E_z(x', y', 0, t) = \frac{1}{2\pi\epsilon_0}\left[\int_{H_1}^{H_2}\frac{2 - 3\sin^2\theta}{R^3}\cdot\int_0^t j(z, t' - R/c)\,\mathrm{d}t'\mathrm{d}z + \int_{H_1}^{H_2}\frac{2 - 3\sin^2\theta}{cR^2}j(z, t - R/c)\,\mathrm{d}z - \int_{H_1}^{H_2}\frac{\sin^2\theta}{c^2R}\frac{\partial j(z, t - R/c)}{\partial t}\,\mathrm{d}z\right]. \tag{31}$$

In this equation, $R = \sqrt{(x')^2 + (y')^2 + (z)^2}$ is the distance from the observation point to dz. The three terms in equation (31) are referred to as the electrostatic, induction, and radiation terms, respectively.

[31] Finally, by matching the simulation results to the data, we can find the RREA-EAS model parameters and the corresponding main properties of the NBP sources.

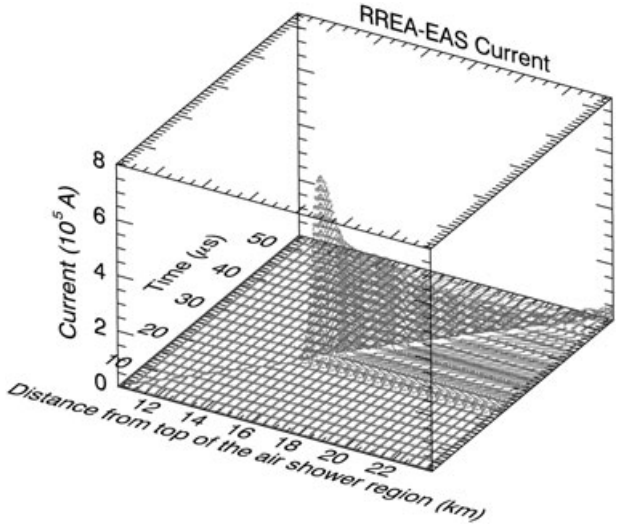

Figure 6. RREA-EAS model predicted current pulse that produced NBP ID 082308_164.

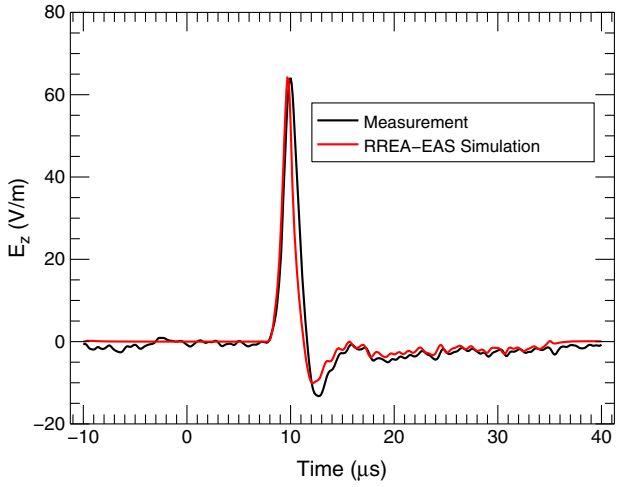

Figure 7. Comparison of measured *E* field waveform to the results from RREA-EAS model simulation.

3.1. Comparison With the Data

[32] We have used the data for three CIDs acquired at the Lightning Observatory in Gainesville, FL, in 2008, which are part of the database consisting of 157 events examined by *Nag et al.* [2010], in order to test the RREA-EAS model. Table 1 shows the properties of these events.

[33] Since the pulses due to these events are all PNBPs in the physics sign convention, the electrostatic field in the cloud is assumed to be downward with electrons as charge carriers moving upward. In the classical picture of a thundercloud, this physical situation can happen between the main negative and the main positive charge centers of the cloud.

[34] NBP ID 082308_163 was a positive NBP, and its source was located at 19 km altitude. It was detected by a ground-based antenna at a distance of 71 km from the source. The measured source height in our simulations has been defined as the altitude at the end of the avalanche region. The magnitude of the electrostatic field inside the cloud, required for this event, can be calculated by the

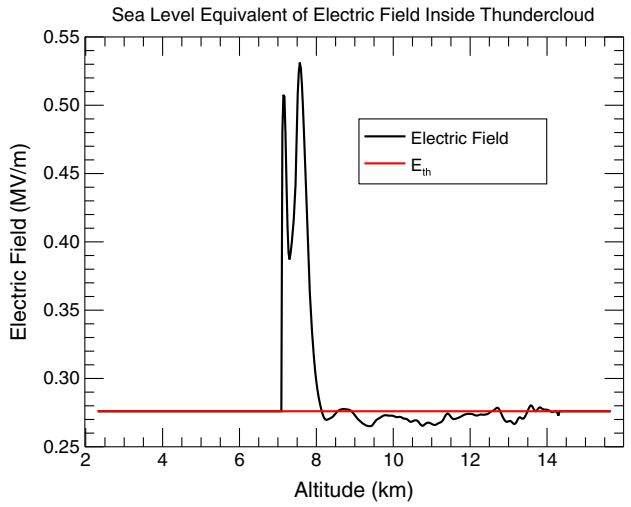

Figure 8. RREA-EAS model predicted electrostatic field inside thundercloud for NBP ID 091108_175.

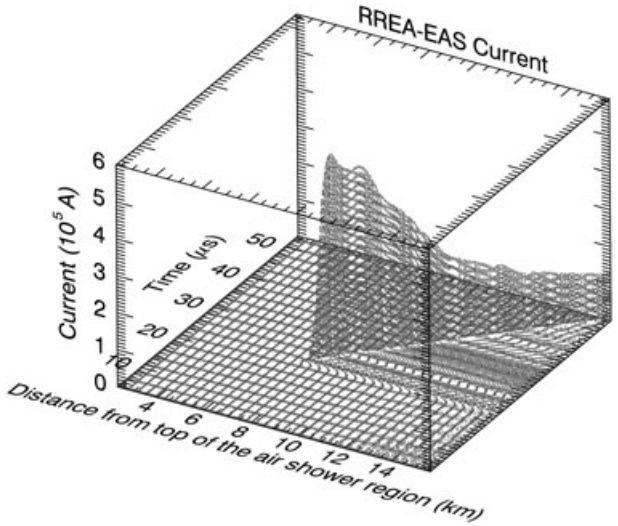

Figure 9. RREA-EAS model predicted current pulse that produced NBP ID 091108_175.

Prediction process described in equation (30). For this event, the transform would result in a field shown in Figure 2.

[35] Figure 2 shows the thundercloud field required to produce the sferic according to the RREA-EAS model. The current due to runaway electrons is calculated using equations (15)–(17). The current due to the low-energy electrons, which trail the runaway electrons, is calculated using equations (18) and (19). Utilizing all these equations, we next simulate the outcome of NBP measurements. Figure 3 shows the current pulse produced by the RREA-EAS process. It has a much smaller width (about 200 ns) than the current pulse in the TL model. This is expected since, in the RREA-EAS model, electrons have a much smaller spatial distribution than in the TL model seen in Figure 1. Finally, Figure 4 shows the comparison of our model prediction with the data. Note that the negative peak of the simulated pulse is a little bit smaller than the measured one. This is due to the approximation we made in our *Prediction* method. In our approximation we ignored the longitudinal diffusion of electrons. However, in the *Correction* part of the model we did not ignore it, and when electrons travel from the region with a field higher than the RREA threshold electric field to the region with a field lower than the threshold electric field, the longitudinal diffusion of the electrons resists any sharp fall in the current pulse. Slower fall in the current pulse would result in a smaller negative peak in the radiation electric field.

[36] The energy of the primary cosmic ray can be calculated from the current pulse produced by the RREA-EAS process (similar to *Dwyer et al.* [2009]). The number of air shower particles is related to the energy of the primary cosmic ray through the empirical relation [*Gaisser*, 1990]:

$$N_{\mathrm{EAS}} \sim 5 \times 10^{-2} E_0^{1.1}, \tag{32}$$

where E_0 is the energy of the cosmic ray measured in GeV. On the other hand, *Dwyer* [2008] showed that due to the relativistic feedback mechanism of runaway electrons there is an upper limit on the avalanche multiplication factor, $\exp(\epsilon) < 10^5$. The size of the avalanche region in the unit of the number of avalanche length is ϵ. This relation shows that

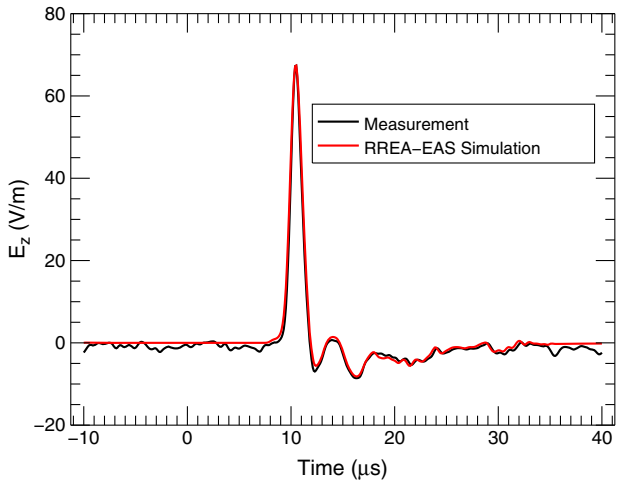

Figure 10. Comparison of measured E field waveform to the results from RREA-EAS model simulation.

the number of generated electrons from each air shower seed particle is less than 10^5 electrons. Using these two empirical relations we are able to find the minimum energy of the primary cosmic ray for any number of avalanche electrons:

$$E_0 > \left(\frac{N_e}{5 \times 10^{-2} \times 10^5} \right)^{1/1.1} \text{[GeV]}, \tag{33}$$

where N_e is the total number of electrons at the end of the avalanche region. The number of electrons, N_e, could be calculated using the magnitude of the current at the end of the avalanche region:

$$N_e(z) = \int_0^\infty \frac{J(z,t')S(z - v_{\text{re}}t')}{e} \mathrm{d}t', \tag{34}$$

where $S(z - v_{\text{re}}t')$ is the step function

$$S(z - v_{\text{re}}t') = \begin{cases} 1 & z - v_{\text{re}}t' > 0 \\ 0 & z - v_{\text{re}}t' < 0 \end{cases}, \tag{35}$$

and e is the charge of electron. The minimum cosmic ray energy required to produce a pulse similar to NBP ID 082308_163 is about 6.06×10^{21} eV (see Table 2). This is too high an energy for any incoming cosmic ray particle. We will talk more about this in the discussion section.

[37] We also tested the RREA-EAS model for two more measurements listed in Table 1. The observed characteristics of these pulses, NBP ID 082308_164 and 091108_175, are given in Table 1. Figures 5 and 8 show the required sea level equivalent electric field inside the thundercloud based on the RREA-EAS theory. The required electrostatic fields are again found from the same *Prediction* process used before. The multipeak electrostatic field for NBP ID 091108_175 shows how the electric field inside the thundercloud should approximately look like for the case of the NBPs with multiple secondary peaks (oscillations). *Nag and Rakov* [2009, 2010a] interpreted these multiple peaks in terms of bouncing current pulse in a conductive channel. The corresponding current pulses are shown in Figures 6 and 9. Figure 6 is the current pulse for NBP ID 082308_164, and Figure 9 is for NBP ID 091108_175. The current pulses include the realistic contributions of both attachment and diffusion inside the thundercloud. The model-predicted radio pulses are overlaid with the actual measurements in Figures 7 and 10. The minimum energies of the primary cosmic ray for these two events have also been estimated and given in Table 2.

4. Discussion and Conclusions

[38] Although our RREA-EAS model results can be forced to match the radio observations, the inferred thunderstorm and cosmic ray properties are probably not realistic. The primary cosmic rays required by the RREA-EAS have to have energies not observed before. Based on our simulations, the minimum energy of the cosmic ray should be about $\sim 10^{21}$ eV. These energies are much higher than the Greisen-Zatsepin-Kuzmin limit for cosmic rays from distant sources ($\sim 10^{20}$ eV). The spectrum of the cosmic rays on Earth with energies higher than 3×10^6 GeV can be estimated by the following analytical expression [*Berezinskii et al.*, 1984]:

$$I_{\text{c.r.}}(E) = 3 \times 10^{-10} (E(\text{GeV})/10^6)^{-2.1} \text{ particles/cm}^2 \text{ s sr}. \tag{36}$$

Using this equation, we can see that the occurrence of a cosmic ray particle with the energy of about 10^{21} eV during a thunderstorm of the size 100 km^2 is one particle for every 67 years. In case of weaker NBPs, the frequency of the cosmic ray particles with energies of about 1 order of magnitude smaller, 10^{20} eV, is about one particle in every 6 months. These occurrence frequencies are much less than the frequency of the observation of NBPs which can be several or more per storm (see *Lü et al.* [2013] for a recent review).

[39] Moreover, RREA-EAS probably requires nonphysical or at least extremely high electric fields inside the thundercloud.

[40] We also found different values for some previously known properties of NBEs. The speed of the electrical discharge in the RREA-EAS process is the same for all CIDs and it is about $0.89c$, where c is the speed of light. This is close to the upper bound of the range reported by other researchers [see *Nag and Rakov*, 2010a, and references therein]. A different value for the speed of the discharge could also affect other inferred characteristics of CIDs, such as the length of the discharge channel. It has been inferred that the length of discharge channels for CIDs are less than 1 km [*Smith et al.*, 1999; *Nag and Rakov*, 2010a]. However, based on our results, at least for the three simulations we have presented here, the discharge channel lengths were about 13.2 km, 13.3 km, and 7.88 km (see Table 2). These lengths are on the order of the size of a thundercloud and are too long even for normal intracloud discharges (vertical extent only).

[41] Another discrepancy between our RREA-EAS results and the results from other models is the maximum discharge current. It has been estimated by the TL model that the electric discharge current pulse in a CID would reach the maximum of a few hundreds of kiloamperes [*Nag and Rakov*, 2010b, Figure 7]. In our simulations the electric discharge current peaks (see Table 2) are all in excess of 500 kA, which is larger than previously estimated values. Such a disparity could be explained by the fact that in most CID models the *current moment* is the measurable property and the actual magnitude of the currents could have different values, depending on assumed channel length. The

30–100 kA [*Gurevich et al.*, 2004] value of peak current was based on having a wide current pulse over a short distance in space. However, in the RREA-EAS model, we are dealing with a very sharp current pulse which travels a long distance in space. Both of these views would result in the same current moment change.

[42] As a final note, *Gurevich et al.* [2004] mistakenly use the statistical data of the fall+rise time (not the total time) of NBPs mentioned in *Smith et al.* [2002] as the total duration of the signal for these events in order to show that the RREA-EAS process is the underlying mechanism for CIDs. NBPs have a total duration of 10–30 μs [*Smith et al.*, 1999, 2002; *Nag et al.*, 2010]. The fall+rise time defined in *Smith et al.* [2002] is the time duration of the first half cycle in the bipolar pulse. The total (characteristic) time scale of discharge and pulse duration in a RREA-EAS process is the sum of the "attachment" time of low-energy electrons and the "*e*-folding" rise and then fall times of runaway electrons. The maximum "attachment" time at 13 km in the atmosphere is a bit more than 3 μs [*Morrow and Lowke*, 1997]. The "*e*-folding" time of runaway electrons depends on the electric field in addition to the height of discharge. For the sea level equivalent electric field of 280–350 kV/m at the 13 km altitude the *e*-folding time is about 2.5–4.5 μs. So the total characteristic time scale of discharge and pulse duration is about 5.5–7.5 μs. This is appreciably smaller than the correct total duration of NBPs of 10–30 μs. Note that this is in contrast with the result in *Gurevich et al.* [2004], which suffers from the mistake mentioned above.

[43] The joint process between Relativistic Runaway Electron Avalanche and Extensive Air Showers has long been suggested to be responsible for the production of NBPs. In this paper, we have shown that we can find the fields that reproduce NBP shapes, but these are not realistic for thunderclouds and the required energy of EAS is too high. Furthermore, some of the characteristics of CIDs are model dependent, and no explanation of how VHF emission is produced by CIDs is provided by this model. On the other hand, the TL models also suffer from offering no explanation of the production of the (required) conductive hot channel. Altogether, our results do not support the RREA-EAS hypothesis, as it relates to CIDs.

Appendix A: Green's Function Calculation

[44] The Green's function corresponding to equation (7) should satisfy the following differential equation:

$$\frac{\partial G_{\mathrm{re}}}{\partial t} + \vec{\nabla}\cdot(\vec{v}_{\mathrm{re}}G_{\mathrm{re}}) - \frac{\partial}{\partial z}\left(D_{\parallel}\frac{\partial G_{\mathrm{re}}}{\partial z}\right) - \frac{G_{\mathrm{re}}}{\tau} = \delta(x-x_0)\delta(y-y_0)\delta(z-z_0)\delta(t-t_0). \tag{A1}$$

[45] For the case of constant longitudinal diffusion coefficient, we have

$$G_{\mathrm{re}}(x,y,z,t;x_0,y_0,z_0,t_0) = \frac{1}{\sqrt{4\pi(t-t_0)D_{\parallel}}} \times \exp\left(\int_{t_0}^{t}\frac{\mathrm{d}t}{\tau} - \frac{(v_{\mathrm{re}}(t-t_0)-(z-z_0))^2}{4(t-t_0)D_{\parallel}}\right) \cdot S(t-t_0)S(t-t_0)\delta(x-x_0)\delta(y-y_0)S(z_0)S(L-z). \tag{A2}$$

However, in this paper we are dealing with a nonuniform ambient electric field, and we know that the longitudinal diffusion coefficient depends on the ambient electric field using the following empirical equation [*Dwyer*, 2010]:

$$\frac{D_{\parallel}}{v} = (3.80\times10^{3})E^{-1.57}[\mathrm{m}]. \tag{A3}$$

This dependency prevents us from deriving a simple analytical formula for the Green's function in (A1). However, we can overcome this by assuming the $D_{\parallel}$ to be constant over a very small time interval and treat $\sqrt{4D_{\parallel}\Delta t}$ as an uncertainty in the measurement of a Gaussian distribution. In such a setup, we can find the value of $4D_{\parallel}\Delta t$ at any time using the discrete uncertainties propagation rule [*Taylor*, 1997]:

$$\overline{\sigma} = \sqrt{\sigma_1^2+\sigma_2^2+\cdots}, \tag{A4}$$

we have

$$\overline{\sigma} = \sqrt{4\Delta t D_{\parallel}^1 + 4\Delta t D_{\parallel}^2 + \cdots}. \tag{A5}$$

[46] Since the electrons are moving with approximately constant speed, $t = \frac{z}{t}$, we have

$$\begin{aligned}\overline{\sigma} &= \sqrt{\frac{1}{v}\sum 4\Delta z D_{\parallel}^{i}} \\ &= \sqrt{\frac{z}{v}\frac{\sum 4\Delta z D_{\parallel}^{i}}{z}} \\ &\cong \sqrt{\frac{z}{v}\frac{\int 4\mathrm{d}z D_{\parallel}}{z}} \\ &= \sqrt{4t\overline{D}_{\parallel}},\end{aligned} \tag{A6}$$

where

$$\overline{D}_{\parallel} = \frac{\int D_{\parallel}\mathrm{d}z}{z}. \tag{A7}$$

So at every arbitrary point in space and time, we can rewrite our Green's function for a variable diffusion coefficient as

$$\begin{aligned}G_{\mathrm{re}}(x,y,z,t;x_0,y_0,z_0,t_0) = {} & \frac{1}{\sqrt{4\pi(t-t_0)\overline{D}_{\parallel}(z,z_0)}} \\ & \cdot \exp\left(\int_{t_0}^{t}\frac{\mathrm{d}t}{\tau} - \frac{(v_{\mathrm{re}}(t-t_0)-(z-z_0))^2}{4(t-t_0)\overline{D}_{\parallel}(z,z_0)}\right) \\ & \cdot S(t-t_0)\,S(t-t_0)\,S(z_0)\,S(L-z) \\ & \cdot \delta(x-x_0)\,\delta(y-y_0),\end{aligned} \tag{A8}$$

where

$$\overline{D}_{\parallel}(z,z_0) = \frac{\int_{z_0}^{z} D_{\parallel}\mathrm{d}z}{z-z_0}. \tag{A9}$$

Appendix B: RF Emission From Runaway Breakdown

[47] In *Roussel-Dupré and Gurevich* [1996] and *Tierney et al.* [2005] the peak electric field due to the radio emission from runaway breakdown measured by a distant observer is presented as the following analytical expression in cgs units:

$$E_p = \frac{e\nu}{Rc}\cdot\frac{\beta_r e^{\eta}\sin\theta}{(1-\beta_r\cos\theta)^2}\cdot\left[1+\frac{\langle\varepsilon_r\rangle}{34\ \mathrm{eV}}\cdot\frac{\beta_e}{\beta_r}\cdot\frac{1-\beta_r\cos\theta}{1-\beta_e\cos\theta}\right], \tag{B1}$$

where ν is the avalanche rate, η is the number of *e*-folding of the runaway electrons, θ is the observation angle measured from the direction of the velocity of the runaway electrons, R is the distance to the observer, β_r is the dimensionless speed

of the runaway electrons, β_e is the dimensionless speed of the low-energy electron point charge, and $\langle \varepsilon_r \rangle$ is the mean runaway electron energy. This equation for the radiation field can be separated into two terms:

$$E_p = \frac{e\nu}{Rc} \cdot \frac{e^{\eta} \sin\theta}{(1-\beta_r \cos\theta)} \cdot \left[\underbrace{\frac{\beta_r}{(1-\beta_r \cos\theta)}}_{\text{Term 1}} + \underbrace{\frac{\langle \varepsilon_r \rangle}{34 \text{ eV}} \cdot \frac{\beta_e}{(1-\beta_e \cos\theta)}}_{\text{Term 2}} \right]. \quad \text{(B2)}$$

[48] Based on the speed of the charge used in each term, it can be seen that "Term 1" is the radiation term due to the runaway electrons and "Term 2" is due to the low-energy electrons. The dimensionless speed of low-energy electrons, β_e has been defined as the drift speed of low-energy electrons [*Roussel-Dupré and Gurevich*, 1996].

[49] To see where these two terms come from, consider the vector Liénard-Wiechert potential for a point charge is [*Jackson*, 1999]

$$\vec{A}(\vec{x}, t) = \left[\frac{q\vec{\beta}}{(1-\vec{\beta} \cdot \hat{n})R} \right]_{\text{ret}}. \quad \text{(B3)}$$

[50] In *Roussel-Dupré and Gurevich* [1996] the relativistic electron beam is approximated as a single point charge that its magnitude grows at the avalanche rate ν, $Q_p = -e\, e^{\nu t}$, and it is moving with the constant dimensionless speed β_r. So the radiation electric field due to the point charge at distance R is [*Dwyer et al.*, 2009]

$$\vec{E}_{\text{re}}(\vec{x}, t) = -\frac{\partial \vec{A}_{\text{rad}}(\vec{x}, t)}{\partial t}, \quad \text{(B4)}$$

where

$$\vec{A}_{\text{rad}}(\vec{x}, t) = -\hat{n} \times (\hat{n} \times \vec{A}(\vec{x}, t)). \quad \text{(B5)}$$

So

$$\begin{aligned} \vec{E}_{\text{re}}(\vec{x}, t) &= -\frac{\partial}{\partial t} \left\{ \left[\frac{e\, e^{\nu t} \hat{n} \times (\hat{n} \times \vec{\beta}_r)}{(1-\vec{\beta}_r \cdot \hat{n})R} \right]_{\text{ret}} \right\} \\ &= -\frac{\partial}{\partial t_r} \left\{ \left[\frac{e\, e^{\nu t} \hat{n} \times (\hat{n} \times \vec{\beta}_r)}{(1-\vec{\beta}_r \cdot \hat{n})R} \right]_{\text{ret}} \right\} \cdot \frac{\partial t_r}{\partial t} \\ &= -\left\{ \frac{e\nu e^{\nu t_{\text{ret}}} \hat{n} \times \left(\hat{n} \times \vec{\beta}_r \right)}{(1-\vec{\beta}_r \cdot \hat{n}_{\text{ret}})R_{\text{ret}}} \right\} \cdot \left\{ \frac{1}{(1-\vec{\beta}_r \cdot \hat{n}_{\text{ret}})} \right\} \\ &= -\frac{e\nu}{R_{\text{ret}}} \cdot \frac{e^{\eta} \hat{n} \times (\hat{n} \times \vec{\beta}_r)}{(1-\vec{\beta}_r \cdot \hat{n}_{\text{ret}})^2}. \end{aligned} \quad \text{(B6)}$$

[51] The peak of this radiation field will be

$$E_{\text{re}}(\vec{x}, t) = -\frac{e\nu}{R_{\text{ret}}} \cdot \frac{\beta_r e^{\eta} \sin\theta}{(1-\vec{\beta}_r \cdot \hat{n}_{\text{ret}})^2}, \quad \text{(B7)}$$

which is the term in equation (B2) for the runaway electrons. The low-energy electrons are also represented as a single-point charge whose instantaneous magnitude in the frame of the beam is $Q_s = (\langle \varepsilon_r \rangle / 34 \text{ eV}) Q_p$, and it is moving with the dimensionless drift velocity β_e [*Roussel-Dupré and Gurevich*, 1996]. Similarly with this assumption, the peak radiation electric field of the low-energy electrons at distance R is

$$E_{\text{le}}(\vec{x}, t) = \frac{e\nu}{R_{\text{ret}}} \cdot \frac{e^{\eta}}{(1-\vec{\beta}_r \cdot \hat{n}_{\text{ret}})} \cdot \frac{\langle \varepsilon_r \rangle}{34 \text{ eV}} \cdot \frac{\beta_e \sin\theta}{(1-\vec{\beta}_e \cdot \hat{n}_{\text{ret}})}. \quad \text{(B8)}$$

[52] Then, the total peak radiation electric field from relativistic runaway avalanche is

$$E_{\text{rad}}(\vec{x}, t) = \frac{e\nu}{R_{\text{ret}}} \cdot \frac{e^{\eta} \sin\theta}{(1-\vec{\beta}_r \cdot \hat{n}_{\text{ret}})} \cdot \left[\frac{\beta_r}{(1-\vec{\beta}_r \cdot \hat{n}_{\text{ret}})} + \frac{\langle \varepsilon_r \rangle}{34 \text{ eV}} \cdot \frac{\beta_e}{(1-\vec{\beta}_e \cdot \hat{n}_{\text{ret}})} \right]. \quad \text{(B9)}$$

This is the same expression as equation (B2). This expression overestimates the actual RF electric field at the observation point due to two conceptual errors made in the derivation of this equation which will be explained below.

[53] The first and the main source of the error is in misinterpretation of the propagation velocity of the current from the low-energy electrons. It was assumed that the current due to the low-energy electrons propagates at the drift velocity of these electrons. However, this is a wrong assumption since the individual low-energy electrons quickly attach to the atoms and ions of the air, and their current instead moves at their group velocity which is the same as the runaway electrons [*Dwyer et al.*, 2009].

[54] The second error which has already been discussed in *Dwyer and Babich* [2011] was in the calculation of the ratio of low-energy (secondary) electrons to runaway (primary) electrons ($\frac{n_s}{n_p}$). It was assumed [*Roussel-Dupré and Gurevich*, 1996] that this ratio is

$$\frac{n_s}{n_p} = \frac{Q_s}{Q_p} = \frac{\langle \varepsilon_r \rangle}{34 \text{ eV}}. \quad \text{(B10)}$$

However, *Dwyer and Babich* [2011] have shown that this ratio is actually equal to

$$\frac{n_s}{n_p} = \frac{\eta \tau_a}{\left(1 + \frac{\tau_a}{\tau_{\text{re}}}\right)}, \quad \text{(B11)}$$

where η is the production rate of the low-energy electrons by energetic runaway electrons, τ_a is the attachment time of the low-energy electrons, and τ_{re} is the e-folding time of the runaway electrons. Equations (B10) and (B11) only agree in the limit of very high electric fields where $\tau_{\text{re}} \ll \tau_a$. In any other physical situation, equation (B10) causes extra inaccuracy in the total radiation field of low-energy electrons.

[55] In this appendix we discussed the issues on the model presented in *Roussel-Dupré and Gurevich* [1996] for radiation from the runaway breakdown current. We show that the model overestimates the current produced by the low-energy electrons. This issue has propagated through the literature by using the same assumptions [e.g., *Fullekrug et al.*, 2010; *Gurevich et al.*, 2004].

[56] **Acknowledgments.** This work has been supported in part by the NASA grant NNX12A002H, by DARPA grant HR0011-1-10-1-0061, and by NSF grant ATM-0852869. I wish to thank Samaneh Sadighi for her helpful discussions and comments.

[57] Robert Lysak thanks the reviewers for their assistance in evaluating this paper.

References

Berezinskii, V., S. Bulanov, V. Ginzburg, V. Dogel, and V. Ptuskin (1984), *The Astrophysics of Cosmic Rays* [in Russian], vol. 1, 360 pp., Izdatel'stvo Nauka, Moscow, Russia.

Coleman, L. M., and J. R. Dwyer (2006), Propagation speed of runaway electron avalanches, *Geophys. Res. Lett.*, *33*, L11810, doi:10.1029/2006GL025863.

Dwyer, J. R. (2003), A fundamental limit on electric fields in air, *Geophys. Res. Lett.*, *30*(20), 2055, doi:10.1029/2003GL017781.

Dwyer, J. R. (2005), The initiation of lightning by runaway air breakdown, *Geophys. Res. Lett.*, *32*, L20808, doi:10.1029/2005GL023975.

Dwyer, J. R. (2008), Source mechanisms of terrestrial gamma-ray flashes, *J. Geophys. Res.*, *113*, D10103, doi:10.1029/2007JD009248.

Dwyer, J. R. (2010), Diffusion of relativistic runaway electrons and implications for lightning initiation, *J. Geophys. Res.*, *115*, A00E14, doi:10.1029/2009JA014504.

Dwyer, J. R., and L. P. Babich (2011), Low-energy electron production by relativistic runaway electron avalanches in air, *J. Geophys. Res.*, *116*, A09301, doi:10.1029/2011JA016494.

Dwyer, J. R., and L. Babich (2012), Reply to comment by A. V. Gurevich et al. on "Low-energy electron production by relativistic runaway electron avalanches in air", *J. Geophys. Res.*, *117*, A04303, doi:10.1029/2011JA017487.

Dwyer, J. R., M. A. Uman, and H. K. Rassoul (2009), Remote measurements of thundercloud electrostatic fields, *J. Geophys. Res.*, *114*, D09208, doi:10.1029/2008JD011386.

Dwyer, J. R., D. M. Smith, and S. A. Cummer (2012), High-energy atmospheric physics: Terrestrial gamma-ray flashes and related phenomena, *Space Sci. Rev.*, *173*(1-4), 133–196.

Eack, K. B. (2004), Electrical characteristics of narrow bipolar events, *Geophys. Res. Lett.*, *31*, L20102, doi:10.1029/2004GL021117.

Fullekrug, M., R. Roussel-Dupré, E. M. D. Symbalisty, O. Chanrion, A. Odzimek, O. van der Velde, and T. Neubert (2010), Relativistic runaway breakdown in low-frequency radio, *J. Geophys. Res.*, *115*, A00E09, doi:10.1029/2009JA014468.

Gaisser, T. (1990), *Cosmic Rays and Particle Physics*, Cambridge Univ. Press, Cambridge, U. K.

Gurevich, A. V., and K. P. Zybin (2001), Runaway breakdown and electric discharges in thunderstorms, *Phys. Usp.*, *44*, 1119.

Gurevich, A. V., and K. P. Zybin (2004), High energy cosmic ray particles and the most powerful discharges in thunderstorm atmosphere, *Phys. Lett. A*, *329*(4-5), 341–347.

Gurevich, A. V., L. M. Duncan, Y. V. Medvedev, and K. P. Zybin (2002), Radio emission due to simultaneous effect of runaway breakdown and extensive atmospheric showers, *Phys. Lett. A*, *301*(3-4), 320–326.

Gurevich, A. V., Y. V. Medvedev, and K. P. Zybin (2004), New type discharge generated in thunderclouds by joint action of runaway breakdown and extensive atmospheric shower, *Phys. Lett. A*, *329*(4-5), 348–361.

Gurevich, A. V., et al. (2009), An intracloud discharge caused by extensive atmospheric shower, *Phys. Lett. A*, *373*(39), 3550–3553.

Gurevich, A. V., et al. (2013), Cosmic rays and thunderstorms at the Tien-Shan mountain station, *J. Phys. Conf. Ser.*, *409*, 012234.

Hamlin, T., T. E. Light, X. M. Shao, K. B. Eack, and J. D. Harlin (2007), Estimating lightning channel characteristics of positive narrow bipolar events using intrachannel current reflection signatures, *J. Geophys. Res.*, *112*, D14108, doi:10.1029/2007JD008471.

Jackson, J. (1999), *Classical Electrodynamics*, John Wiley & Sons, New York.

Le Vine, D. M. (1980), Sources of the strongest RF radiation from lightning, *J. Geophys. Res.*, *85*(C7), 4091–4095.

Lü, F., B. Zhu, H. Zhou, V. A. Rakov, W. Xu, and Z. Qin (2013), Observations of compact intracloud lightning discharges in the northernmost region (51°N) of China, *J. Geophys. Res. Atmos.*, *118*, 4458–4465, doi:10.1002/jgrd.50295.

Morrow, R., and J. J. Lowke (1997), Streamer propagation in air, *J. Phys. D: Appl. Phys.*, *30*, 614.

Nag, A., and V. A. Rakov (2009), Electromagnetic pulses produced by bouncing-wave-type lightning discharges, *IEEE Trans. Electromagn. Compat.*, *51*(3), 466–470.

Nag, A., and V. A. Rakov (2010a), Compact intracloud lightning discharges: 1. Mechanism of electromagnetic radiation and modeling, *J. Geophys. Res.*, *115*, D20102, doi:10.1029/2010JD014235.

Nag, A., and V. A. Rakov (2010b), Compact intracloud lightning discharges: 2. Estimation of electrical parameters, *J. Geophys. Res.*, *115*, D20103, doi:10.1029/2010JD014237.

Nag, A., V. A. Rakov, D. Tsalikis, and J. A. Cramer (2010), On phenomenology of compact intracloud lightning discharges, *J. Geophys. Res.*, *115*, D14115, doi:10.1029/2009JD012957.

Rakov, V. A., and M. A. Uman (2004), Lightning: Physics and effects, *Phys. Today*, *57*(12), 63–64.

Roussel-Dupré, R., and A. V. Gurevich (1996), On runaway breakdown and upward propagating discharges, *J. Geophys. Res.*, *101*(A2), 2297–2312.

Smith, D. A., X. M. Shao, D. N. Holden, C. T. Rhodes, M. Brook, P. R. Krehbiel, M. Stanley, W. Rison, and R. J. Thomas (1999), A distinct class of isolated intracloud lightning discharges and their associated radio emissions, *J. Geophys. Res.*, *104*(D4), 4189–4212.

Smith, D. A., K. B. Eack, J. Harlin, M. J. Heavner, A. R. Jacobson, R. S. Massey, X. M. Shao, and K. C. Wiens (2002), The Los Alamos sferic array: A research tool for lightning investigations, *J. Geophys. Res.*, *107*(D13), 4183, doi:10.1029/2001JD000502.

Smith, D. A., M. J. Heavner, A. R. Jacobson, X. M. Shao, R. S. Massey, R. J. Sheldon, and K. C. Wiens (2004), A method for determining intracloud lightning and ionospheric heights from VLF/LF electric field records, *Radio Sci.*, *39*, RS1010, doi:10.1029/2002RS002790.

Taylor, J. (1997), *An Introduction to Error Analysis: The Study of Uncertainties in Physical Measurements*, Univ. Sci. Books, Herndon, Va.

Thomas, R. J., P. R. Krehbiel, W. Rison, T. Hamlin, J. Harlin, and D. Shown (2001), Observations of VHF source powers radiated by lightning, *Geophys. Res. Lett.*, *28*(1), 143–146.

Tierney, H. E., R. A. Roussel-Dupré, E. M. D. Symbalisty, and W. H. Beasley (2005), Radio frequency emissions from a runaway electron avalanche model compared with intense, transient signals from thunderstorms, *J. Geophys. Res.*, *110*, D12109, doi:10.1029/2004JD005381.

Uman, M. (2001), *The Lightning Discharge*, Dover, Mineola, N. Y.

Uman, M. A., D. K. McLain, and E. P. Krider (1975), The electromagnetic radiation from a finite antenna, *Am. J. Phys.*, *43*(1), 33–38.

Watson, S. S., and T. C. Marshall (2007), Current propagation model for a narrow bipolar pulse, *Geophys. Res. Lett.*, *34*, L04816, doi:10.1029/2006GL027426.

Willett, J. C., J. C. Bailey, and E. P. Krider (1989), A class of unusual lightning electric field waveforms with very strong high-frequency radiation, *J. Geophys. Res.*, *94*(D13), 16,255–16,267.

Wu, T., W. Dong, Y. Zhang, T. Funaki, S. Yoshida, T. Morimoto, T. Ushio, and Z. Kawasaki (2012), Discharge height of lightning narrow bipolar events, *J. Geophys. Res.*, *117*, D05119, doi:10.1029/2011JD017054.

Zhu, B., H. Zhou, M. Ma, F. Lv, and S. Tao (2010), Estimation of channel characteristics of narrow bipolar events based on the transmission-line model, *J. Geophys. Res.*, *115*, D19105, doi:10.1029/2009JD012021.